Supplemental Figure 1 Progression of ileitis in TNFΔARE mice from 4- to 20-weeks-of-age.

(A) Inflammatory indices from ilea of 4-, 8- and 20-week-old TNFΔARE$^{+/-}$ mice (Mean ± SEM n=12-20). (B) Representative micrographs of ilea at indicated ages; (H&E, 10x magnification, bars=100μm).

Supplemental Figure 2 Partial deficiency of CX_3CR1 did not alter the severity of ileitis.

(A) Inflammatory indices from ilea of 20-week-old TNFΔARE/$CX_3CR1^{+/+}$ and TNFΔARE/$CX_3CR1^{GFP/+}$ mice (Mean ± SEM n=9, 6). (B) Representative micrographs; (H&E, 10x magnification, bars=100μm).

Supplemental Figure 3 Increased CX_3CR1 mRNA transcripts in ilea of TNFΔARE mice.

Analysis of CX_3CR1 mRNA transcripts from 4- and 20-week-old WT and TNFΔARE ileal whole tissues Mean ± SEM, for n=6, *p<0.05).

Supplemental Figure 4 Inclusion of F4/80$^+$ leukocytes did not alter the ratio of CX_3CR1^+ and CD103$^+$ mononuclear phagocytes in chronic ileitis.

The proportion of CD103$^+$ and CX_3CR1^+ cells, without exclusion of F4/80$^+$ cells, were assessed by flow cytometry from the LP of TNFΔARE/$CX_3CR1^{GFP/+}$ and WT/$CX_3CR1^{GFP/+}$ mice at 20-weeks-of-age compared with WT age-matched control mice. (Mean ± SEM, n=4, *p<0.05, **p<0.01).

Supplemental Figure 5 Most CD11c$^+$/CD11b$^+$ mononuclear phagocytes express CX_3CR1 in WT and TNFΔARE/$CX_3CR1^{GFP/+}$ mice.

The fraction of CX_3CR1^+ cells was analyzed by flow cytometry within the CD11c$^+$/CD11b$^+$ MP subset. Representative zebra plots and histograms.

Supplemental Figure 6 CD103$^+$ DC express higher levels of RA synthetic enzymes.

Analysis of RALDH2 mRNA transcripts from isolated $CD11c^{+}/MHCII^{+}$ $CD103^{+}$ and $CD103^{Neg}$ MP from the MLN and LP of 20-week-old mice using GAPDH as an endogenous control (Mean ± SEM, n=6, *p<0.05).

Supplemental Figure 7 Effect of Flt3-L administration on RALDH2 and CX_3CR1 mRNA transcripts in terminal ilea of TNFΔARE mice.

Analysis of RALDH2 and CX_3CR1 mRNA transcripts from whole ileal LP of 20-week-old TNFΔARE mice treated with vehicle or Flt3-L using GAPDH as an endogenous control (Mean ± SEM, n=6, *p<0.05).

Supplemental Figure 8 Effect of Flt3-L administration on the frequency of $E\text{-cadherin}^{+}$ DC isolated from terminal ilea of TNFΔARE mice.

(A) Quantification of $CD11c^{Hi}/MHCII^{+}/E\text{-cadherin}^{+}$ DC from ileal LP of 20-week-old WT and TNFΔARE mice treated with vehicle or Flt3-L (Mean ± SEM, n=4, *p<0.05, ***p<0.001). (B) Representative overlaid histograms of the expression of E-cadherin on $CD11c^{Hi}/MHCII^{+}$ cells from the ileal lamina propria of 20-week-old mice. White histogram indicates WT cells, grey histogram represents vehicle-treated TNFΔARE mice and hatched histogram reflects expression in TNFΔARE mice after treatment with Flt3-L.

Supplemental Figure 9 Effect of Anti-CD25 antibody administration on Flt3-L mediated attenuation of ileitis.

Inflammatory indices from ilea of 20-week-old TNFΔARE mice treated with vehicle, Flt3-L or anti-CD25 antibody + Flt3-L were assessed as described[55] (Mean ± SEM, **p<0.01, *p<0.05, n=5/treatment group).

Figure S1.

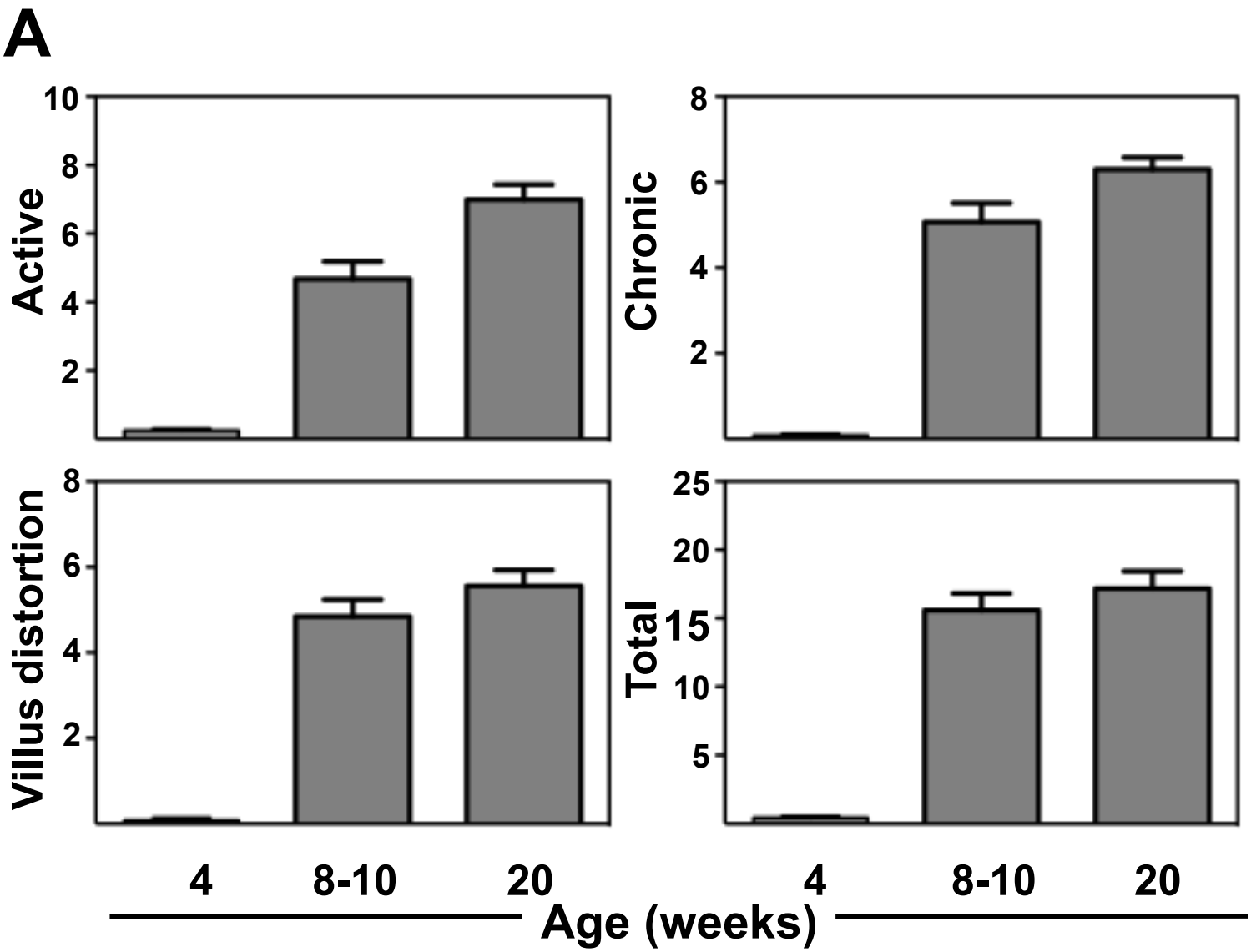
A
Active
Chronic
Villus distortion
Total
10
8
6
4
2
25
20
15
5
4
8-10
20
Age (weeks)

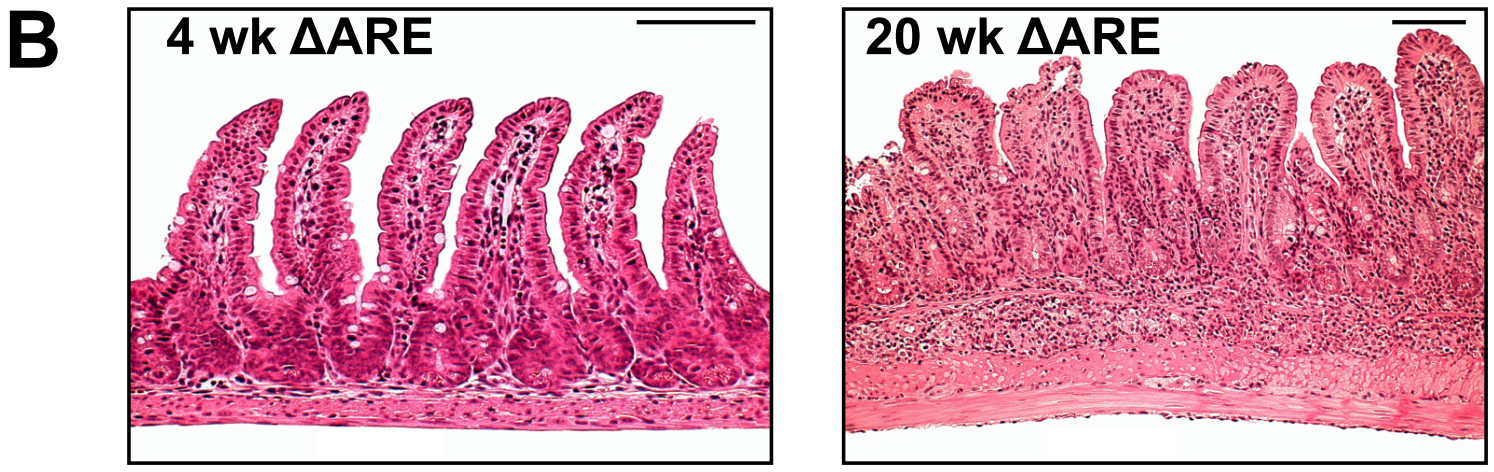
B
4 wk ΔARE
20 wk ΔARE

Figure S2.

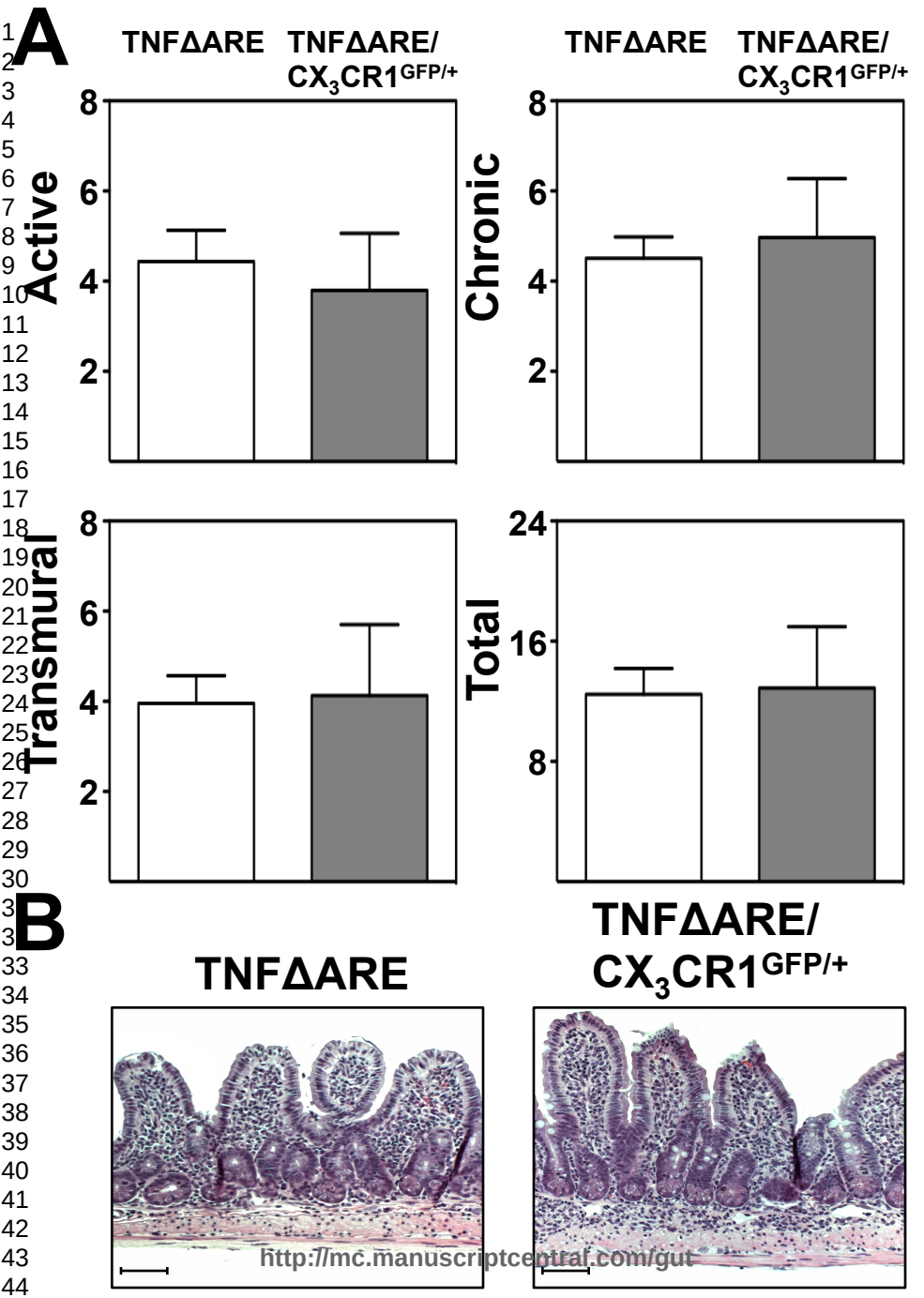

Figure S3.

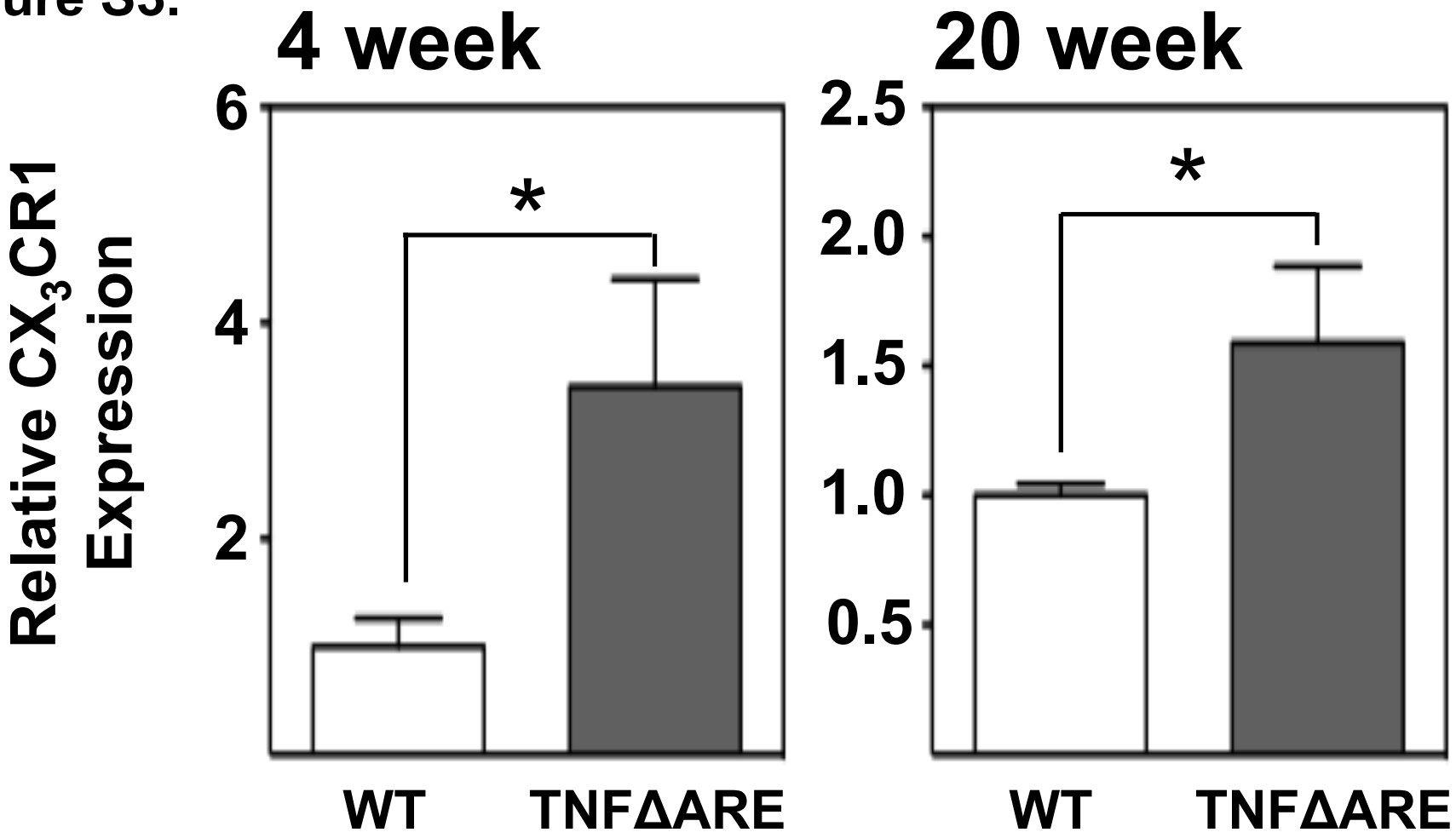
4 week
20 week
Relative CX3CR1 Expression
6
4
2
2.5
2.0
1.5
1.0
0.5
*
*
WT
TNFΔARE
WT
TNFΔARE

Figure S4.

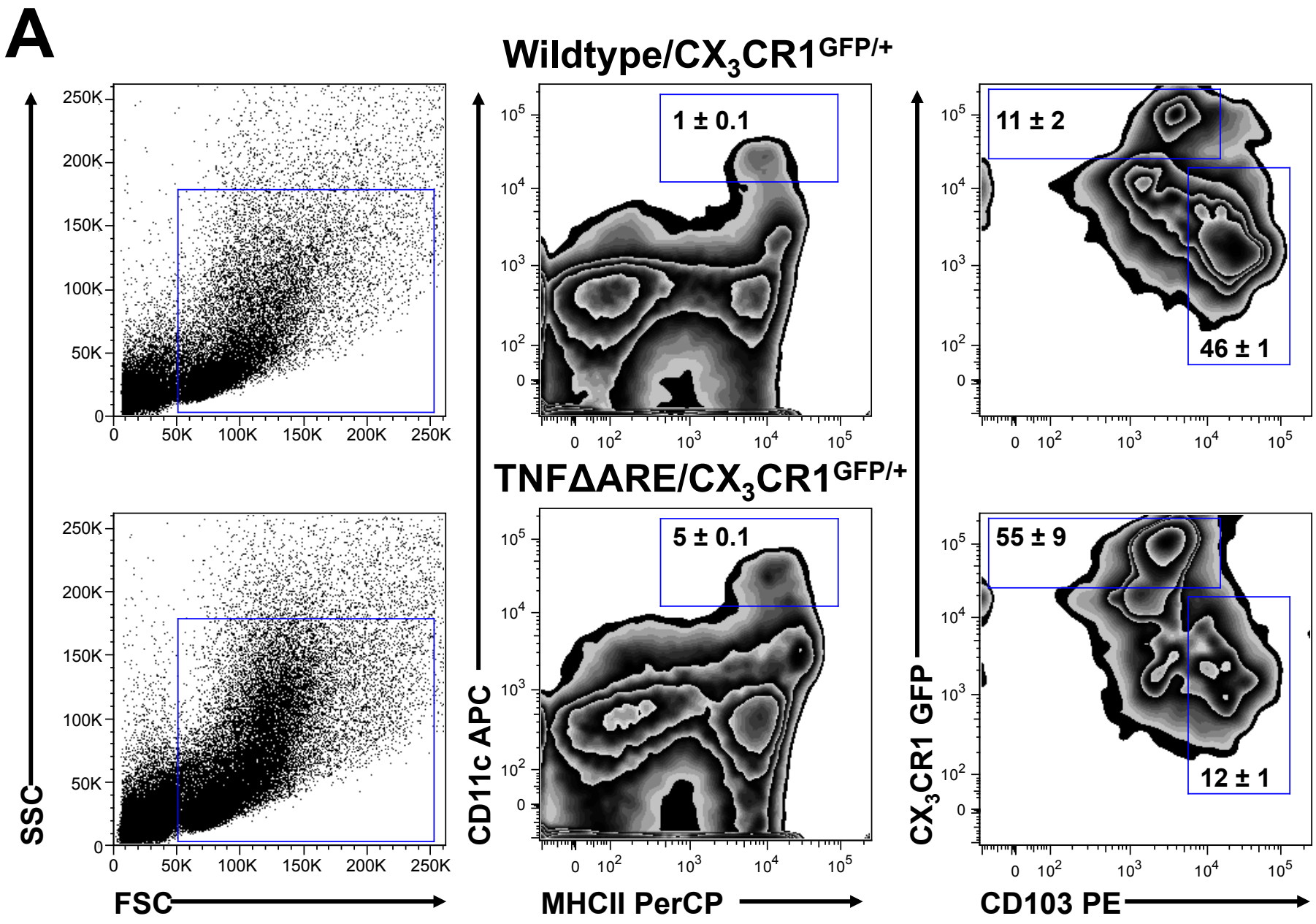
A
Wildtype/CX3CR1GFP/+
TNFΔARE/CX3CR1GFP/+
1 ± 0.1
11 ± 2
46 ± 1
5 ± 0.1
55 ± 9
12 ± 1
SSC
FSC
CD11c APC
MHCII PerCP
CX3CR1 GFP
CD103 PE

Figure S5.

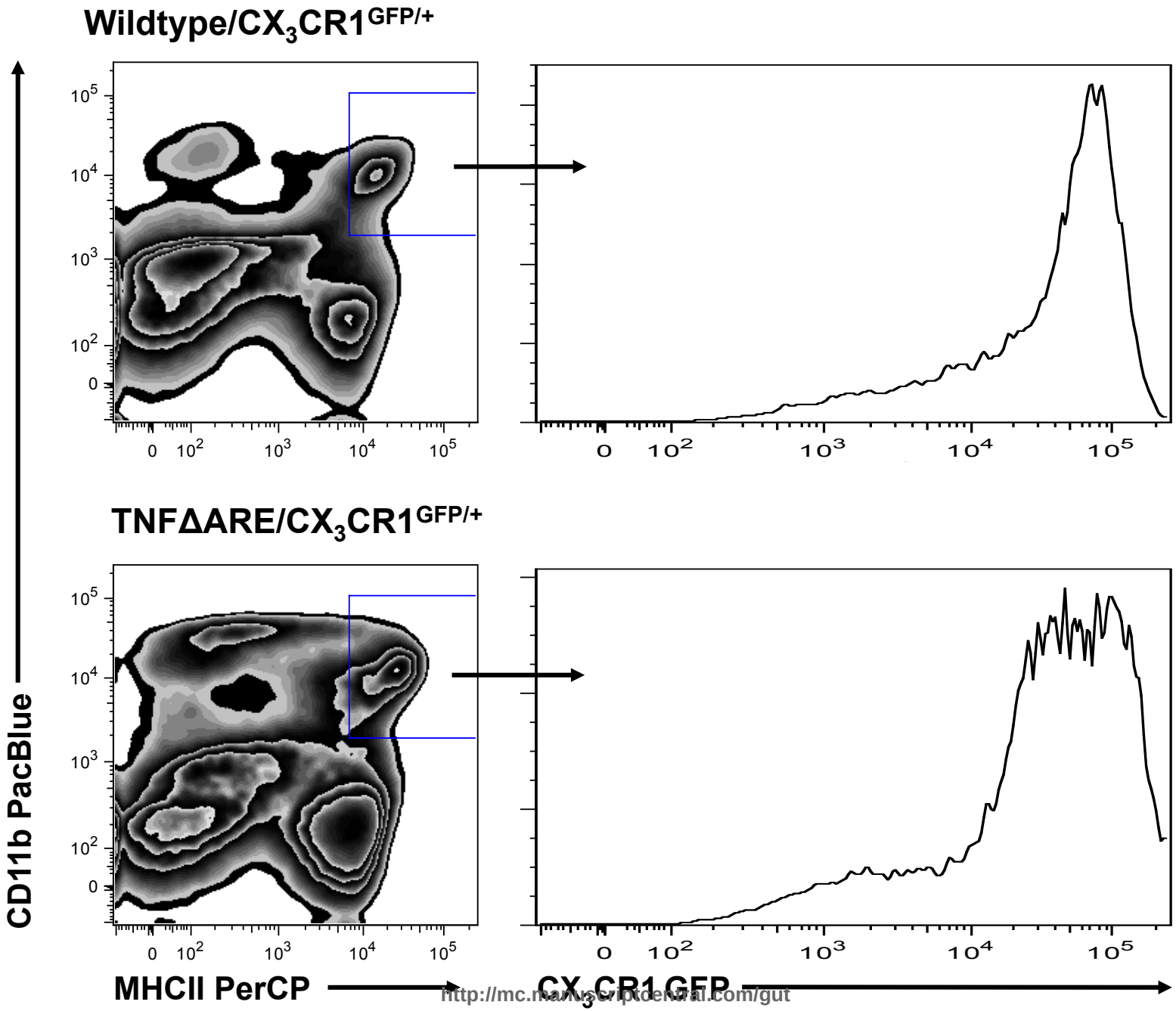

Figure S6.

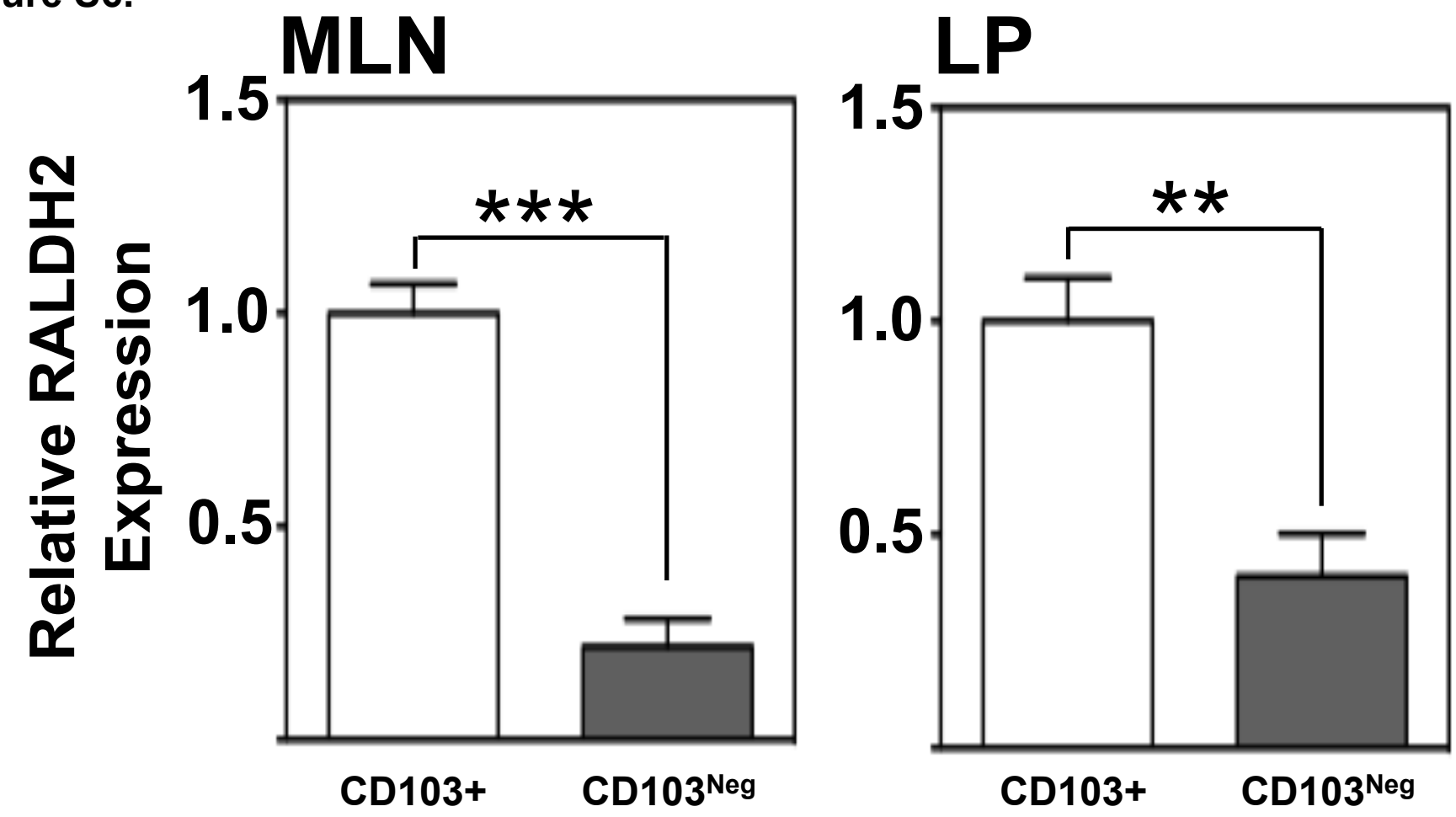
MLN
LP
Relative RALDH2 Expression
1.5
1.0
0.5
***
**
CD103+
CD103Neg
CD103+
CD103Neg

Figure S7.

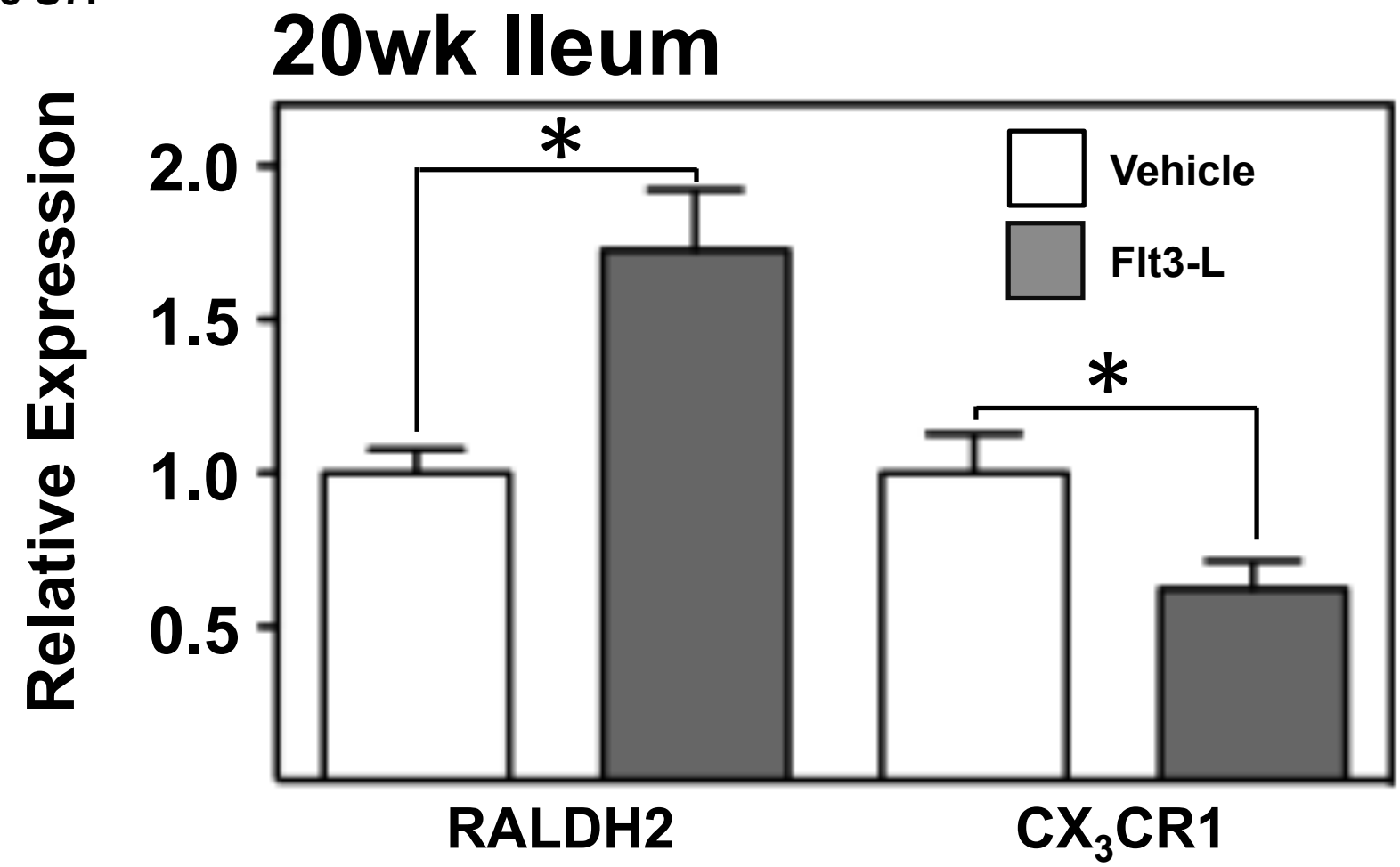
20wk Ileum
Relative Expression
2.0
1.5
1.0
0.5
*
*
Vehicle
Flt3-L
RALDH2
CX3CR1

Figure S8.

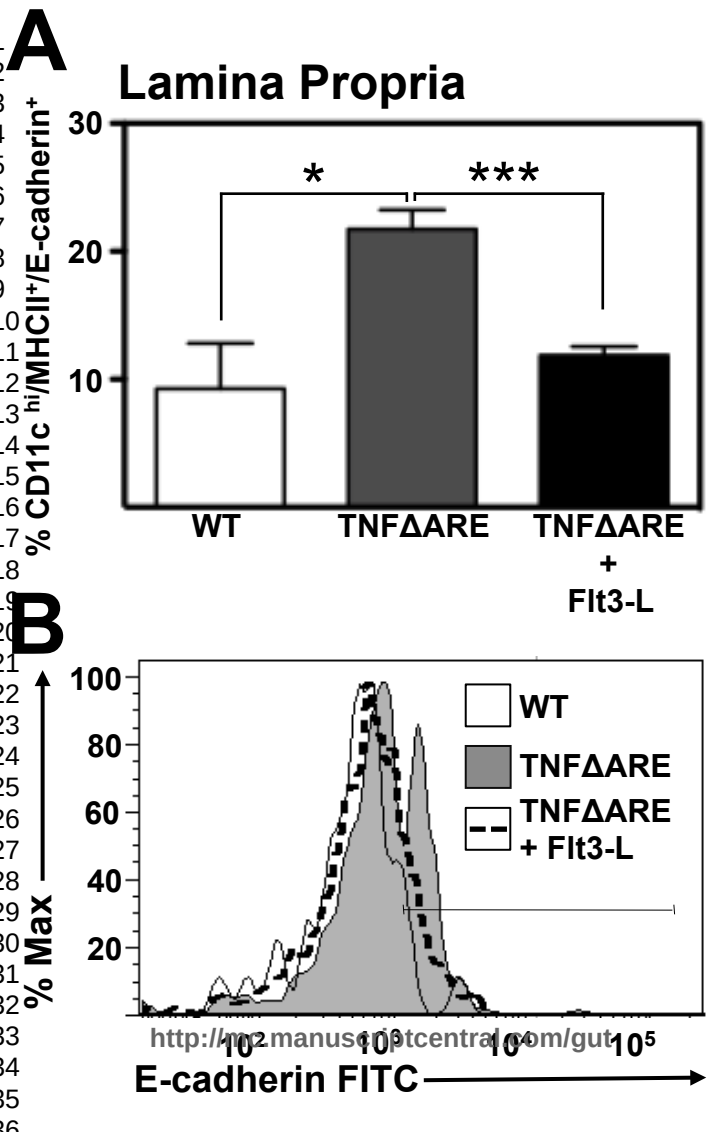

Figure S9